catalysts

Article

The Adsorptive and Photocatalytic Performance of Granite and Basalt Waste in the Discoloration of Basic Dye

Lariana N. B. Almeida [1,*], Tatiana G. Josue [2], Othavio H. L. Nogueira [2], Laura S. Ribas [2], Maria E. K. Fuziki [1], Angelo M. Tusset [3], Onelia A. A. Santos [1] and Giane G. Lenzi [1]

1 Department of Chemical Engineering, State University of Maringá, Maringá 87020-900, Brazil
2 Department of Chemical Engineering, Federal University of Technology–Paraná, Ponta Grossa 84017-220, Brazil
3 Department of Engineering, Federal University of Technology–Paraná, Ponta Grossa 84017-220, Brazil
* Correspondence: beraldolariana@gmail.com

Abstract: The present work explored the adsorptive capacity and catalytic activity of rock powders from basaltic and granitic rocks in the discoloration of synthetic and industrial effluents containing the yellow dye Basic Yellow 96. The rock powders were characterized with scanning electron microscopy associated with energy-dispersive spectroscopy, photoacoustic spectroscopy, N_2 physisorption and X-ray diffraction, the latter confirming the abundant presence of silica in the four materials studied. The basaltic powders presented specific surface areas between 7 and 10 times greater than those of granitic materials, which allowed up to 92% removal of the dye in 3 h of test using the basaltic powder. Despite the smaller area, the granitic materials showed considerable photocatalytic activity in 3 h, 94%, the same as that of the basaltic materials in the photocatalysis. Granitic and basaltic photocatalysts proved to be efficient in the discoloration of synthetic and industrial effluents, although TOC analyses indicated that it was not possible to promote the pollutant mineralization in the industrial effluent. Both artificial light and sunlight were effective in the photocatalysis of the dye, although the former was slightly faster.

Keywords: adsorption; photocatalysis; rock powders; dye removal

check for updates

Citation: Almeida, L.N.B.; Josue, T.G.; Nogueira, O.H.L.; Ribas, L.S.; Fuziki, M.E.K.; Tusset, A.M.; Santos, O.A.A.; Lenzi, G.G. The Adsorptive and Photocatalytic Performance of Granite and Basalt Waste in the Discoloration of Basic Dye. *Catalysts* **2022**, *12*, 1076. https://doi.org/10.3390/catal12101076

Academic Editor: Antonio Eduardo Palomares

Received: 1 September 2022
Accepted: 17 September 2022
Published: 20 September 2022

1. Introduction

In Brazil, several companies exploit rocks in order to sell crushed stones to be used in the paving and civil construction sectors, among others. One of the by-products generated from this activity is rock dust, which has a diversified granulometry, having applications in agriculture and civil engineering. The generated volume of these by-products, however, is much larger than the sold volume, so that the excess of these materials in the quarries leads companies to seek alternative purposes for rock dust.

Igneous rocks, which are those formed from the cooling process of magma or lava, are the main rocks exploited in Brazil. They are formed predominantly by silicon dioxide (SiO_2), and depending on the amount of this oxide, the rocks are classified as acidic (>63%), intermediate (between 52 and 63%), mafic or basic (between 45 and 52%), or ultrabasic (<45%) [1]. Aside from the mineralogical compositions of the magmas, igneous rocks may also differ depending on cooling processes. If the lava extravasated cools naturally on the Earth's surface, it forms an extrusive or plutonic rock, e.g., basalt, but if magma cools still within the Earth's crust at great depths, it produces an intrusive igneous rock, e.g., granite [2]. Basalt is abundantly found in nature, covering 70% of the Earth's surface [3]. It is characterized by a fine grain, with a color that varies from gray to black. Its applications are very diversified, for instance in the manufacture of slabs and tubes [4], as a natural remineralizer for agriculture [5], and in the production of industrial floors and paving [6]. Separately, quartz is the most important phase of silica, constituting, together with other minerals, approximately 12% (by weight) of the earth's crust. It is often found in intrusive igneous rocks such as granite [7].

The presence of organic pollutants, such as dyes, in wastewater is a matter of concern due to the possible damage that these compounds can cause to the environment and populations [8,9]. Given this situation, different technologies have been applied to remove organic contaminants from water, such as adsorption or advanced oxidation processes (AOPs). In adsorption, a solid called an adsorbent under optimal conditions adsorbs on its surface the target pollutant present in a fluid without degrading it, while in AOPs, highly oxidative radicals are generated that are responsible for degrading organic pollutants. In this context, different oxidative processes have already proven to be quite efficient for dye removal [8,9]. In particular, among AOPs, heterogenous photocatalysis has shown promising results, both in organics removal and metals reduction [10]. In heterogeneous photocatalysis, the electronic transitions of a semiconductor electrons are induced through the incidence of artificial or natural radiation, so that oxidation and reduction reactions may take place, removing the pollutant from water.

Different oxides, both pure and combined, have already been applied as photocatalysts, allowing the degradation of pollutants like pharmaceuticals and dyes [11–15]. Silica-based materials, mainly zeolites, have already been used as photocatalysts and as a support for various catalysts containing, for example, nickel and nickel-ruthenium [16], iron [17], calcium oxide [18]. Applications of these catalysts include the treatment of effluent decontamination, removal of pollutants, organic [19], palladium, molybdenum and zirconium [20], and dye adsorbents [21]. The use of rock dust in the discoloration treatment of solutions containing dye by adsorption and photocatalysis is also innovative and contributes value to the material since in the literature, there are not many studies that use natural materials as catalysts. In one such study, Salcedo et al. [22] used Bojuru sand in the photocatalytic degradation of phenolic compounds. Basaltic rock has good characteristics for adsorbents, i.e., their low cost, large surface area and large volume availability, ref. [23]. Some studies have already used it for this purpose, such as in the adsorption of chromium (VI) [23], nickel [24], carbon dioxide [25] and also as a catalyst in Fenton and photo-Fenton reactions for the oxidation of cationic dyes [3].

In this sense, the present study aimed to evaluate the use of rock dust as an adsorbent and photocatalyst in the treatment of decolorization of synthetic and industrial effluent. The adsorptive and photocatalytic potential of basalt and granite rock powders was evaluated in the discoloration treatment of industrial effluent containing Basic Yellow 96 dye. The latter was selected as the target pollutant of this study since dyes are complex organic compounds, generally used to improve the appearance of food, fabrics, packaging [26]. There are more than 10,000 types of synthetic dyes applied to different industrial sectors such as: textiles, pulp and paper, leather, pharmaceuticals, cosmetics. In addition, it is estimated that more than 1,000,000 tons of dyes are used annually. These materials are often leached into nature and can cause damage to ecosystems. This has caused great concern and raised the search for strategies that overcome the challenges related to environmental contamination by synthetic dyes [26].

2. Results

2.1. Characterization Results

The catalysts' surface characterizations obtained with the SEM/EDS analyses are shown in Figure 1. Some elements were present in all the four materials: O, Si, Al, Na, K, Fe, and Ca. O and Si were the most abundant elements in the four samples. Thus, it can be said that most of the materials are basically made of silica, which is characteristic of granitic and basaltic rocks. The presence of silicon, aluminum, and oxygen characterizes the materials as aluminosilicate minerals. The materials are distinguished by the concentration of these and other elements, such as K, Fe, and Na.

(**a**)

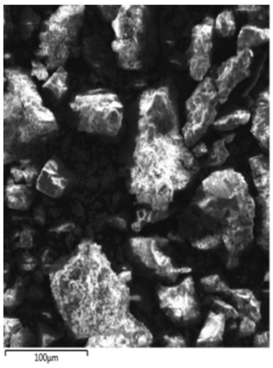

Map Sum Spectrum		
	Wt%	σ
O	53.5	0.2
Si	25.7	0.2
Al	6.6	0.1
Fe	5.1	0.1
K	3.5	0.1
Na	2.6	0.1
Ca	2.0	0.1
Mg	0.9	0.1
Ti	0.2	0.1

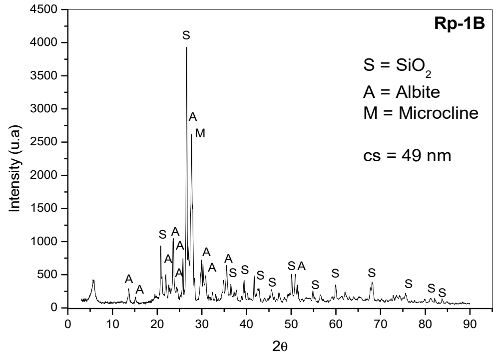

(**b**)

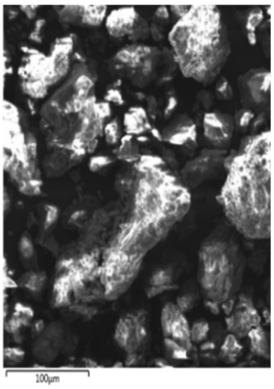

Map Sum Spectrum		
	Wt%	σ
O	52.1	0.1
Si	19.2	0.1
Fe	11.3	0.1
Al	6.3	0.0
Ca	5.0	0.0
Mg	2.9	0.0
Na	1.7	0.0
Ti	0.8	0.0
K	0.5	0.0
Mn	0.2	0.0

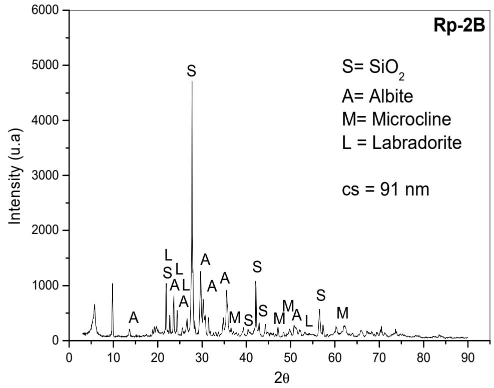

(**c**)

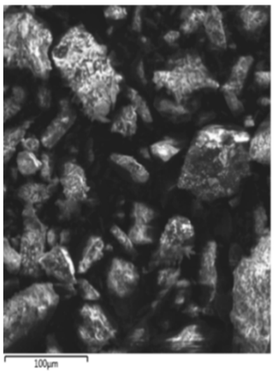

Map Sum Spectrum		
	Wt%	σ
O	54.9	0.2
Si	29.2	0.1
Al	6.8	0.1
Na	4.1	0.1
K	3.0	0.1
Fe	1.4	0.1
Ti	0.3	0.0
Ca	0.3	0.0

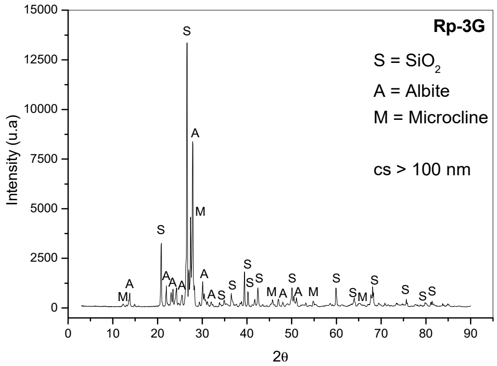

(**d**)

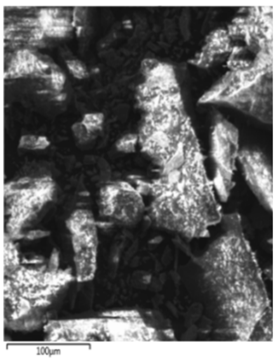

Map Sum Spectrum		
	Wt%	σ
O	55.8	0.2
Si	30.4	0.2
Al	5.7	0.1
Na	3.5	0.1
K	2.8	0.1
Fe	1.2	0.1
Ca	0.6	0.1

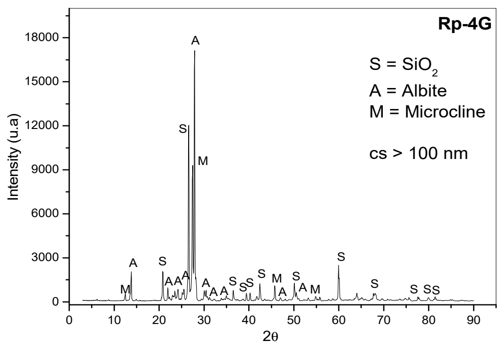

Figure 1. SEM-EDS and XRD (500×) results for each material studied: (**a**) Rp-1B, (**b**) Rp-2B, (**c**) Rp-3G, and (**d**) Rp-4G.

Figure 1 also presents the XRD results, which indicated the presence of SiO_2, Albite and Microcline phases in the four samples, and also Labradorite phase in Rp-2B sample.

One aspect that differentiates granites from basalts can be observed in the specific surface area (S_0) results, presented in Table 1, while the granites presented a very small S_0, the basaltic rock powders have a surface area up to 7 to 10 times greater than the granitic powders, which reflects in the volume of pores and in the average diameter of pores as well. In turn, the four materials presented very similar values of band gap energy (E_{gap}) and absorption wavelength (λ) (Table 1). This probably results from the predominant presence of silicon in the same crystalline phases in the four materials identified in the XRD and EDS.

Table 1. Values of S_0, Vp, dm, Egap and λ of the samples.

	S_0 (m^2/g)	Vp (cc/g)	dm (Å)	Egap (eV)	λ (nm)
Rp-1B	8.5	0.024	111	2.25	551
Rp-2B	15	0.036	97	2.27	546
Rp-3G	1.5	0.007	200	2.16	574
Rp-4G	1.6	0.005	131	2.21	561

Adsorption-desorption isotherms (Figure 2) show that the four materials can be considered as mesopores, being respectively similar to type 4 and type 5 isotherms.

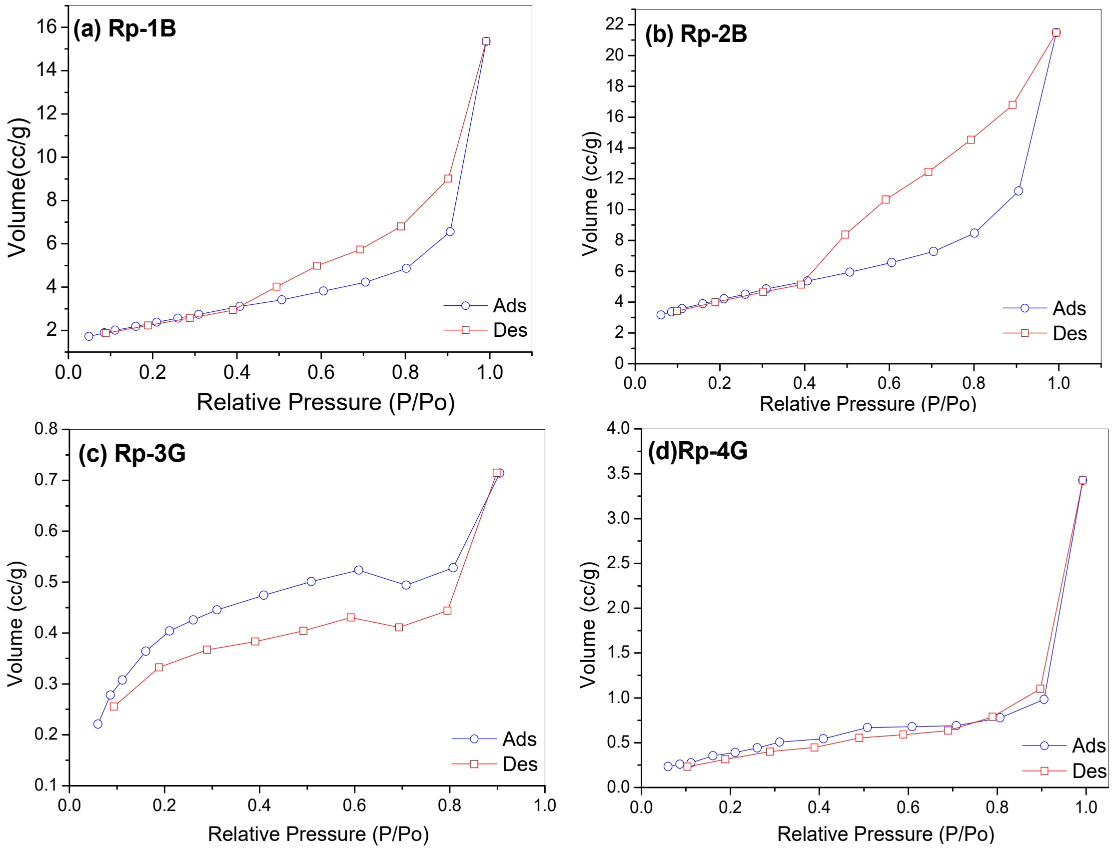

Figure 2. N_2 adsorption and desorption isotherms: (**a**) Rp-1B, (**b**) Rp-2B, (**c**) Rp-3G and (**d**) Rp-4G.

2.2. Photocatalytic Tests Results

The experimental tests started with the treatment of synthetic effluent. Figure 3 illustrates the results obtained from this first stage in which all four rock powders were tested. From a general perspective, the four stone powders showed good photocatalytic activity in discoloration the synthetic solution. However, basalt powders (Rd-1B and Rd-2B) also had a considerable role as adsorbents, and Rd-B2 was an even better adsorbent than catalyst. The results show that it would be possible to use any of the rock powders for the color treatment of the synthetic solution since all of them reached a percentage close to 94% of discoloration, at the end of 3 h of reaction either by adsorption or photocatalysis.

After the experimental tests with synthetic effluent (Figure 3), it was identified that for a better treatment of the industrial effluent, adsorption followed by photocatalysis should be combined. Rp-3G and Rp-2B were selected as the materials with the best performance in the treatment of the synthetic effluent. Thus, they were used in the treatment of the molded pulp packaging industry effluent. The catalyst concentration was 6.0 g L^{-1}, and no adjustment was made to the effluent pH. Tests were performed using artificial radiation and natural radiation (Figure 4).

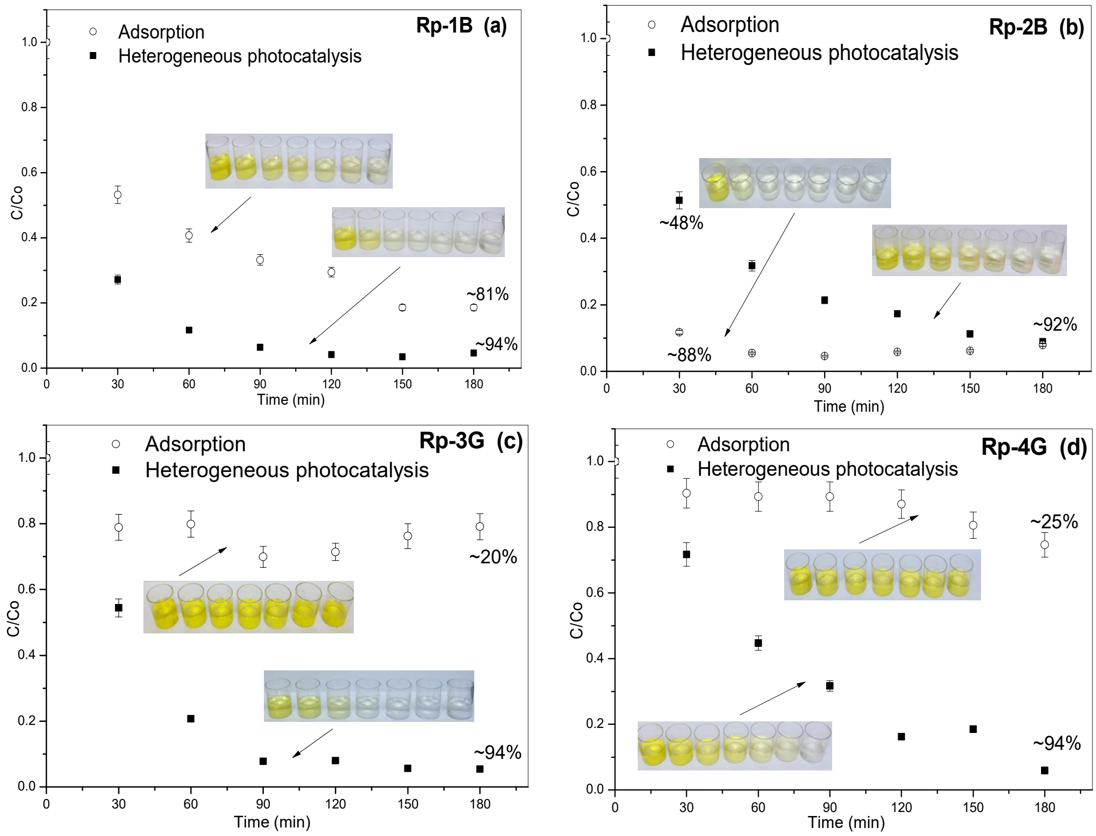

Figure 3. Results of discoloration of the synthetic solution in 3 h. Treatment of synthetic effluent by adsorption and photocatalysis with (**a**) Rp-1B, (**b**) Rp-2B, (**c**) Rp-3G and (**d**) Rp-4G. Error bars represent the standard deviation of measurements for the tests.

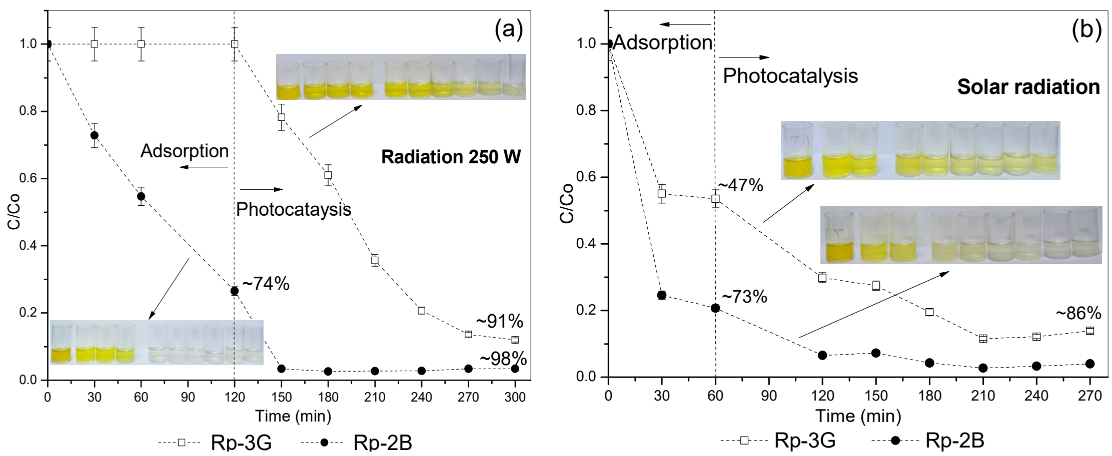

Figure 4. Results of the discoloration test using the industrial effluent: (**a**) artificial radiation (250 W vapor lamp) and (**b**) solar radiation. Error bars represent the standard deviation of measurements for the tests.

The radiant energy intensities during the test are presented in Figure 5. In Table 2, the characterization of distilled water and effluents (synthetic and industrial) is presented.

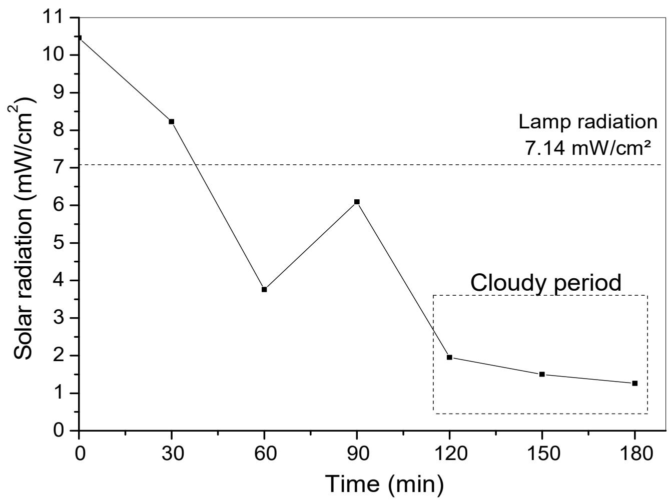

Figure 5. Artificial radiation and solar radiation irradiation intensity during experimental tests with industrial effluent.

Table 2. Characterization of distilled water, synthetic effluent, and industrial effluent before and after the reactions.

	Distilled Water	Synthetic Solution	IE before	IE after Pr-2B	IE after Pr-2B and Solar Radiation	IE after Pr-3G	IE after Pr-3G and Solar Radiation
COD (mg L^{-1})	13	21	170	85	100	96	95
BOD (mg L^{-1})	4	5	60	43	56	53	53
TOC (mg L^{-1})	<5	<5	25	18	25	25	25
TSSC (mg L^{-1})	8	9	58	<5	<5	18	<5
NO_3 (mg L^{-1})	<0.5	<0.5	<0.5	<0.5	<0.5	<0.5	<0.5
SURF (mg L^{-1})	<0.5	<0.5	<0.5	<0.5	<0.5	<0.5	<0.5

The values must be multiplied by 10. IE = Industrial effluent.

3. Discussion

As a general observation, there is a similarity in the four diffractograms and in the crystalline phases identified (Figure 1). The two granitic powders (Rp-3G and Rp-4G) had very similar diffractograms, and the same phases were identified: silica, albite and microcline. The other two basaltic rock powders (Rp-1B and Rp-2B) also presented these compounds, however, Rp-2B also presented labradorite, which was mentioned by Schiavon, Redondo and Yoshida [4] as one of the frequent components of basaltic rock.

In a separate analysis of the rocks, it can be seen that basaltic powders (Rp-1B and Rp-2B) present Fe is in greater concentration than in the granite materials. According Babievskaya et al. [27] basaltic rocks will always contain magnetite ($FeO•Fe_2O_3$) in their composition. In turn, Acar et al. [28] mentioned that the general composition of basaltic rocks is 52.8% SiO_2, 17.5% Al_2O_3, 10.3% Fe_2O_3 and 8.59% CaO. Schiavon et al. [4] described that basalt is a very abundant volcanic rock on Earth, being composed of silicon, aluminum and iron minerals, in the forms of augite (pyroxene), labradorite (plagioclase) and magnetite.

Another difference observed in XRD characterization (Figure 1) is the size of the crystallites. The two granitic powders (Rp-3G and Rp-4G) presented sizes (cs) greater than 100 nm, while the basaltic rock powders, Rp-1B and Rp-2B, presented, respectively, 49 nm and 91 nm, the former being the smallest crystallite size among the four materials. Possibly due the cooling happens very quickly, the crystals are generally smaller in comparison to granite, as it has a slower cooling, which provides and facilitates the crystallization of minerals.

Regarding the specific surface area of the materials (Table 1), it was observed that basaltic catalysts presented a larger specific area in comparison to the granitic material.

Hwang et al. [25] studied a zeolite produced from basalt and applied it as a carbon dioxide (CO_2) adsorbent. In the zeolite characterization, they observed an area of 19 m^2/g and a pore volume equal to 0.05 cm^3/g, values that are close to those of Rp-2B, which was, among the four materials, the one with the highest specific area and greater pore volume.

Having a larger specific area increases the probability of adsorption of the pollutant on the surface of the adsorbent/catalyst. It was reflected directly in the removal efficiency by adsorption (Figure 3) of the basaltic materials, which presented higher removal percentages (81% for Rp-1B and 93% for Rp-2B).

Granite from ornamental rocks rich in iron has already been used as a Fenton catalyst in dye degradation, however there was no considerable adsorption of dye in the research conducted by Ferreira et al. [29]. In the heterogeneous photocatalysis tests, in turn, the granitic materials showed results as promising as those of basaltic materials, reaching 94% removal after 3 h of testing (Figure 3).

A common characteristic of all the presently studies materials was the large amount of silica in their composition. On the other hand, the biggest difference between the four materials was the S_0 value: basaltic powders presented considerably larger S_0. Although the adsorption also depends on operational variables such as pH and initial concentration of pollutant, the size of the specific surface area of the adsorbent is a crucial factor, given that dye molecules are generally large, and, since it is essentially a surface phenomenon, the greater the surface area, the greater availability for adsorption. In addition, basalt proved to be more versatile than granite, as it presented good results both as an adsorbent and as a catalyst. Recent studies have already shown that basalt, after being used as an adsorbent, can be incorporated in the manufacture of bricks [30].

Rp-2B proved to be an excellent adsorbent, both in the tests performed with synthetic (Figure 3) and the industrial effluent (Figure 4). Furthermore, the combination of adsorption followed by photocatalysis provided a remarkable color change after the incidence radiation, both artificial and natural.

Rp-2B achieved greater and faster effluent discoloration when compared to Rp-3G. This behavior is probably related to the greater specific area of Rp-2B (10× greater than Rp-3G), which promoted a greater adsorption of the dye on the surface of Rp-2B, favoring the degradation of the adsorbed pollutant by photogenerated hydroxyl radicals when subjected to artificial or natural radiation.

Ziolli and Jardim [31] describe that the hydroxyl radical photogenerated through the electron-hole pair can act in several ways to attack the pollutant molecule, for example: it can attack a molecule present in solution, it can be released from the surface of the semiconductor and migrate, as a free radical, into the solution and can also diffuse across the surface of the adsorbent and react with the adsorbate (adsorbed molecule). Supposedly, this last hypothesis mentioned by Ziolli and Jardim in 1998 [31] may have happened with Rp-2B and the dye in industrial effluent.

It is worth mentioning that, with artificial radiation, the discoloration was much faster and the solution was extremely clear in the first 30 min of photocatalysis, which would justify stopping the reaction, since the percentage of discoloration remained constant until the end of 300 min.

In the tests performed with solar radiation (Figure 4b), the discoloration was slower, however, on the day of this experimental test the weather was partially cloudy (solar radiation in Figure 5) and even so, it can be seen that the solution cleared and remained constant after 120 min of natural radiation.

Almeida et al. [32], when using artificial and natural radiation to degrade caffeine, observed that with the radiation coming from the lamp, there was a faster degradation of the pollutant and this may have happened due to the direction of the incidence of artificial radiation. Furthermore, intervals of cloudy periods can also contributed to this slower degradation of caffeine. Although in the present study there was a similar trend to that found in the study by Almeida et al. [32], that is, better results using artificial radiation, it was noted that both types of radiations could be used for the treatment of effluent. A system was proposed in which it was possible to use both natural and artificial radiation from lamps, when necessary.

Another important factor to be highlighted is the organic composition of industrial effluent (Table 2), which, compared to distilled water and synthetic effluent, has very high COD, BOD and TOC values, which characterizes it as an effluent with high polluting potential if dumped into bodies of water. However, with the reactions with both artificial and solar radiation, it was possible to verify that there was, in addition to the decrease in coloration, a decrease in these parameters, except for the TOC parameter. TOC, in most cases, remained constant, indicating that there was insignificant mineralization of the pollutant, probably due to the formation of by-products [33].

Basalt proved to be very promising for the discoloration of industrial effluent, being an adsorbent/photocatalyst of satisfactory performance, low cost and abundant in quarries, as well as other rock powders. Basalt has already been used, associated with chemical fertilization, as a nutrient source for soybean planting [34], as a Fenton and photo-Fenton catalyst for the discoloration of methylene blue and basic red dye 18 [3], as a chromium VI adsorbent [23], as a nickel adsorbent [8] and now also as an adsorbent/photocatalyst for the Basic Yellow 96 dye present in industrial effluent.

Furthermore, it should be taken into account that this is an initial study on the use of rock powders for the treatment of industrial effluent containing dye, and due to the possible formation of intermediates during the photoreaction, further research is needed to clarify the reaction mechanism, although accessing the molecular structure of the dye is not possible, since it is the property of the manufacturer. However, two advantages can be highlighted: the low cost and the large volume available of material, in addition to the easy execution of the reaction proposed here.

4. Materials and Methods

In this research, four materials were used as catalysts, two basaltic rock powders and two granitic rock powders. The materials were acquired from four different quarries located in the states of Paraná and São Paulo, Brazil. Figure 6 shows the locations where samples were collected as well as photographs of each material.

Figure 6. Rock powders used in the research. Rock exploration locations where samples were collected.

4.1. Characterizations of the Catalysts

Materials were characterized by: scanning electron microscopy (SEM) associated with energy dispersive spectroscopy (EDS), photoacoustic spectroscopy, N_2 physisorption, and X-ray diffraction (XRD).

4.1.1. Scanning Electron Microscopy-Energy Dispersive Spectroscopy

The SEM and EDS characterizations were performed using a scanning electron microscope model VEGA3 LMU–Tescan, equipped with retractable SE and BSE detectors, low vacuum (500 Pa) and motorized with movements on the x, y and z axes. The EDS detector coupled to the same equipment as the MEV is of the AZTec Energy X-Act model, resolution 130 eV–Oxford. The equipment is at Federal University of Technology Paraná, Ponta Grossa, PR- Brazil.

4.1.2. Photoacoustic Spectroscopy

In order to carry out the photoacoustic spectroscopy characterization, a combination of equipment was made following the sequence of a radiation source emitting energy to a mechanical modulator that then passes through a monochromator, filters and reaches the photoacoustic cell, where the sample and the microphone, which emits a signal that is captured by a synchronized amplifier and which subsequently provides the intensity and phase of the photoacoustic signal, and this data is then transferred to a computer. The spectra obtained were then normalized in relation to the carbon signal, and the direct band gap energies (E_{gap}) of each material were obtained using the linear method (a linear fit is made in the graph of the square of the absorption coefficient versus the photon energy). The equipment is at Federal University of Technology Paraná, Ponta Grossa, PR- Brazil.

4.1.3. Physisorption of N_2

In this study, the nitrogen (N_2) physisorption method at 77 K was used for this characterization and the equipment used was the Quantachrome Autosorb Automated Gas Sorption System. The specific area was calculated using the B.E.T method, and the pore volume and the average pore diameter determined at a relative pressure of 0.99 by the BJH method. The equipment is at Federal University of Santa Catarina, Florianópolis, SC- Brazil.

4.1.4. X-ray Diffraction

For the XRD analysis, a Rigaku diffractometer, model MiniFlex300/600, with conditions of 40 kV, 15 mA from 30 to 90 deg was used. The equipment is at Federal University of Technology Paraná, Pato Branco, PR- Brazil.

4.2. Experimental Photocatalytic Tests

The experimental tests were initially carried out with a synthetic dye solution and distilled water and, then, after defining the two catalysts with the best performance, experimental tests were carried out with industrial effluent from the molded pulp packaging industry, located in the Campos Gerais region, Paraná, Brazil.

Regarding the experimental tests, a yellow liquid dye Basic Yellow 96 was used as a pollutant, the same dye used to dye the packaging in the industry where the industrial effluent was collected. Synthetic solutions were made with distilled water at a dye concentration of 10 $\mu L\ L^{-1}$. The wavelength used in the UV-Vis spectrophotometer (Fento 800VI) to determine the residual concentrations of dye throughout the reaction was 430 nm.

For heterogeneous photocatalysis tests, the reaction system was equipped with a borosilicate reactor, magnetic stirrer, cooling jacket for passing cold water and air flow at a flow rate of 0.5 L min^{-1}. The light source used was a 250 W mercury vapor lamp (irradiance: 7.14 mW/cm^2), which was attached above the reactor. As for the adsorption tests, the reaction system consisted of a borosilicate reactor and a magnetic stirrer, with no radiation source.

The pH of the reaction medium was maintained without adjustments, and the adsorbent/catalyst concentration was 1 g L^{-1} for synthetic solution and 6.0 g L^{-1} of catalyst for industrial effluent, conditions defined in previous research [35]. A photolysis test was also carried out in which the system had a reactor, stirrer, cooling jacket and lamp. In this test, only the influence of radiation on the discoloration of the solution was verified, without the presence of the catalyst. In order to evaluate the use of solar radiation, and following the same procedures described above, experimental tests were also carried out using natural radiation and, to measure the radiant energy intensity, a Sentry radiometer model ST-513 was used.

4.3. Characterization of the Industrial Effluent

After the experimental tests with the synthetic effluent made with water and dye, tests were carried out with the industrial effluent from the molded pulp packaging industry that also contained the same Basic Yellow 96 dye added during the packaging production. The effluent was then collected, stored in a plastic container, and kept under refrigeration for carrying out the experimental tests in the laboratory. The effluent was characterized using Pastel UV–Secomam equipment, in which it was possible to obtain information on biological oxygen demand (BOD), chemical oxygen demand (COD), total organic carbon (TOC), total soluble solids content (TSSC), surfactants and nitrate of nitrogen N (NO_3).

5. Conclusions

In this study, we investigated the application of waste rock powders (basaltic and granitic), from four different locations, as adsorbents and photocatalysts in the discoloration of synthetic and industrial effluent containing Basic Yellow 96 dye.

Basalt and granite stone powders were efficient in the discoloration of the solution. The basaltic materials stood out in the adsorption process, reaching values of 81% (Rp-1B) and 92% (Rp-2B) of removal in three hours of testing. Granite powders, despite the low removal by adsorption (between 20 and 25%), obtained good results in the photocatalysis tests, reaching about 94% removal. The great difference between the basaltic and granitic materials in the adsorption performance can be attributed to the higher specific surface areas of the basalt powders, which were about 7 to 10 times greater than those of the granite powders.

Discoloration was possible in both synthetic and industrial effluent with the use of artificial (lamp) and natural (sun) light. However, TOC results indicated that it was not possible to achieve industrial effluent mineralization.

Despite that, considering the easy execution of the reactions, the lack of heat treatment or preparation of the materials, as well as the large volume of these rock powders generated by quarries in Brazil, the reaction system proposed here characterizes the materials as attractive for the treatment of dyes that contain water. The results also indicated that there is still much be investigated regarding the mechanism involved in the process, as well as the improvement of the pollutant mineralization.

Author Contributions: L.N.B.A., T.G.J., O.H.L.N., L.S.R. and M.E.K.F., carried out the methodology and investigation; A.M.T., O.A.A.S. and G.G.L., conceived of the project and shared in the writing, reviewing and editing. All authors have read and agreed to the published version of the manuscript.

Funding: This research received no external funding.

Data Availability Statement: The data used to support the findings of this study are included within the article. Should further data or information be required, these are available from the corresponding author upon request.

Acknowledgments: The authors acknowledge the CAPES, FA and CNPq, both Brazilian research funding agencies. The fifth author thanks CNPq for the financial support (Process: 310562/2021-0). This study was conducted using the equipment of the C^2MMa UTFPR.

Conflicts of Interest: The authors declare that there are no conflicts of interest regarding the publication of this paper.

References

1. Haldar, S.K. *Introduction to Mineralogy and Petrology*, 2nd ed.; Elsevier: Amsterdam, The Netherlands, 2020; ISBN 9780323851367.
2. Haldar, S.K.; Tišljar, J. Igneous Rocks. In *Introduction to Mineralogy and Petrology*; Elsevier: Amsterdam, The Netherlands, 2014; pp. 93–120. ISBN 9780124081338.
3. Saleh, M.A.; Bilici, Z.; Kaya, M.; Yalvac, M.; Arslan, H.; Yatmaz, H.C.; Dizge, N. The Use of Basalt Powder as a Natural Heterogeneous Catalyst in the Fenton and Photo-Fenton Oxidation of Cationic Dyes. *Adv. Powder Technol.* **2021**, *32*, 1264–1275. [CrossRef]
4. Schiavon, M.A.; Redondo, S.U.A.; Yoshida, I.V.P. Caracterização Térmica e Morfológica de Fibras Contínuas de Basalto. *Cerâmica* **2007**, *53*, 212–217. [CrossRef]
5. Ramos, C.G.; de Mello, A.G.; Kautzmann, R.M. A Preliminary Study of Acid Volcanic Rocks for Stonemeal Application. *Environ. Nanotechnol. Monit. Manag.* **2014**, *1–2*, 30–35. [CrossRef]
6. Sunny, J.E.; Varghese, R.A.; Sagar, S.; Sujin, P.J.; Kassim, R. Application of Basalt and It's Products in Civil Engineering. *Int. J. Eng. Res.* **2020**, *V9*, 511–515. [CrossRef]
7. Götze, J. Editorial for Special Issue "Mineralogy of Quartz and Silica Minerals". *Minerals* **2018**, *8*, 467. [CrossRef]
8. Hien, N.T.; Nguyen, L.H.; Van, H.T.; Nguyen, T.D.; Nguyen, T.H.V.; Chu, T.H.H.; Nguyen, T.V.; Trinh, V.T.; Vu, X.H.; Aziz, K.H.H. Heterogeneous Catalyst Ozonation of Direct Black 22 from Aqueous Solution in the Presence of Metal Slags Originating from Industrial Solid Wastes. *Sep. Purif. Technol.* **2020**, *233*, 115961. [CrossRef]
9. Karim, M.A.H.; Aziz, K.H.H.; Omer, K.M.; Salih, Y.M.; Mustafa, F.; Rahman, K.O.; Mohammad, Y. Degradation of Aqueous Organic Dye Pollutants by Heterogeneous Photo-Assisted Fenton-like Process Using Natural Mineral Activator: Parameter Optimization and Degradation Kinetics. *IOP Conf. Ser. Earth Environ. Sci.* **2021**, *958*, 012011. [CrossRef]
10. Li, S.; Wang, C.; Cai, M.; Yang, F.; Liu, Y.; Chen, J.; Zhang, P.; Li, X.; Chen, X. Facile Fabrication of TaON/Bi_2MoO_6 Core–Shell S-Scheme Heterojunction Nanofibers for Boosting Visible-Light Catalytic Levofloxacin Degradation and Cr(VI) Reduction. *Chem. Eng. J.* **2022**, *428*, 131158. [CrossRef]
11. Li, S.; Wang, C.; Liu, Y.; Xue, B.; Chen, J.; Wang, H.; Liu, Y. Facile Preparation of a Novel Bi2Wo6/Calcined Mussel Shell Composite Photocatalyst with Enhanced Photocatalytic Performance. *Catalysts* **2020**, *10*, 1166. [CrossRef]
12. Li, S.; Chen, J.; Hu, S.; Wang, H.; Jiang, W.; Chen, X. Facile Construction of Novel Bi_2WO_6/Ta_3N_5 Z-Scheme Heterojunction Nanofibers for Efficient Degradation of Harmful Pharmaceutical Pollutants. *Chem. Eng. J.* **2020**, *402*, 126–165. [CrossRef]
13. Li, S.; Hu, S.; Jiang, W.; Zhang, J.; Xu, K.; Wang, Z. In Situ Construction of WO3 Nanoparticles Decorated Bi2MoO6 Microspheres for Boosting Photocatalytic Degradation of Refractory Pollutants. *J. Colloid Interface Sci.* **2019**, *556*, 335–344. [CrossRef] [PubMed]
14. Li, S.; Hu, S.; Jiang, W.; Liu, Y.; Zhou, Y.; Liu, J.; Wang, Z. Facile Synthesis of Cerium Oxide Nanoparticles Decorated Flower-like Bismuth Molybdate for Enhanced Photocatalytic Activity toward Organic Pollutant Degradation. *J. Colloid Interface Sci.* **2018**, *530*, 171–178. [CrossRef] [PubMed]
15. Li, S.; Shen, X.; Liu, J.; Zhang, L. Synthesis of Ta_3N_5/Bi_2MoO_6 Core–Shell Fiber-Shaped Heterojunctions as Efficient and Easily Recyclable Photocatalysts. *Environ. Sci. Nano* **2017**, *4*, 1155–1167. [CrossRef]
16. Paviotti, M.A.; Faroldi, B.M.; Cornaglia, L.M. Ni-Based Catalyst over Rice Husk-Derived Silica for the CO_2 Methanation Reaction: Effect of Ru Addition. *J. Environ. Chem. Eng.* **2021**, *9*, 105173. [CrossRef]
17. Peron, D.V.; Barrios, A.J.; Taschin, A.; Dugulan, I.; Marini, C.; Gorni, G.; Moldovan, S.; Koneti, S.; Wojcieszak, R.; Thybaut, J.W.; et al. Active Phases for High Temperature Fischer-Tropsch Synthesis in the Silica Supported Iron Catalysts Promoted with Antimony and Tin. *Appl. Catal. B* **2021**, *292*, 120141. [CrossRef]
18. Lani, N.S.; Ngadi, N.; Inuwa, I.M. New Route for the Synthesis of Silica-Supported Calcium Oxide Catalyst in Biodiesel Production. *Renew Energy* **2020**, *156*, 1266–1277. [CrossRef]
19. Zeb, S.; Ali, N.; Ali, Z.; Bilal, M.; Adalat, B.; Hussain, S.; Gul, S.; Ali, F.; Ahmad, R.; khan, S.; et al. Silica-Based Nanomaterials as Designer Adsorbents to Mitigate Emerging Organic Contaminants from Water Matrices. *J. Water Process Eng.* **2020**, *38*, 101675. [CrossRef]
20. Wu, H.; Kim, S.-Y.; Miwa, M.; Matsuyama, S. Synergistic Adsorption Behavior of a Silica-Based Adsorbent toward Palladium, Molybdenum, and Zirconium from Simulated High-Level Liquid Waste. *J. Hazard. Mater.* **2021**, *411*, 125136. [CrossRef]
21. Huang, C.-H.; Chang, K.-P.; Ou, H.-D.; Chiang, Y.-C.; Wang, C.-F. Adsorption of Cationic Dyes onto Mesoporous Silica. *Microporous Mesoporous Mater.* **2011**, *141*, 102–109. [CrossRef]
22. Salcedo, G.M.; Kupski, L.; de Oliveira Arias, J.L.; Barbosa, S.C.; Primel, E.G. Bojuru Sand as a Novel Catalyst for Refinery Wastewater Treatment and Phenol Degradation by Heterogeneous Photo Catalysis. *J. Photochem. Photobiol. A Chem.* **2020**, *402*, 112796. [CrossRef]
23. Alemu, A.; Lemma, B.; Gabbiye, N.; Alula, M.T.; Desta, M.T. Removal of Chromium (VI) from Aqueous Solution Using Vesicular Basalt: A Potential Low Cost Wastewater Treatment System. *Heliyon* **2018**, *4*, e00682. [CrossRef] [PubMed]
24. Park, J.H.; Lee, J.K. Weathered Sand of Basalt as a Potential Nickel Adsorbent. *Processes* **2020**, *8*, 1238. [CrossRef]
25. Hwang, K.-J.; Choi, W.-S.; Jung, S.-H.; Kwon, Y.-J.; Hong, S.; Choi, C.; Lee, J.-W.; Shim, W.-G. Synthesis of Zeolitic Material from Basalt Rock and Its Adsorption Properties for Carbon Dioxide. *RSC Adv.* **2018**, *8*, 9524–9529. [CrossRef] [PubMed]
26. Omeje, K.O.; Nnolim, N.E.; Ezema, B.O.; Ozioko, J.N.; Eze, S.O.O. Synthetic Dyes Decolorization Potential of Agroindustrial Waste-Derived Thermo-Active Laccase from Aspergillus Species. *Biocatal. Agric. Biotechnol.* **2020**, *29*, 101800. [CrossRef]
27. Babievskaya, I.Z.; Drobot, N.F.; Fomichev, S.V.; Krenev, V.A. Calculation of the Mineral Composition of Basaltic Rocks. *Inorg. Mater.* **2009**, *45*, 916–918. [CrossRef]

28. Acar, V.; Cakir, F.; Alyamaç, E.; Seydibeyoğlu, M.Ö. Basalt Fibers. In *Fiber Technology for Fiber-Reinforced Composites*; Elsevier: Amsterdam, The Netherlands, 2017; pp. 169–185.
29. Ferreira, S.A.D.; Donadia, J.F.; Gonçalves, G.R.; Teixeira, A.L.; Freitas, M.B.J.G.; Fernandes, A.A.R.; Lelis, M.F.F. Photocatalytic Performance of Granite Waste in the Decolorization and Degradation of Reactive Orange 122. *J. Environ. Chem. Eng.* **2019**, *7*, 103144. [CrossRef]
30. Sanad, S.A.; Abel Moniem, S.M.; Abdel-Latif, M.L.; Hossein, H.A.; El-Mahllawy, M.S. Sustainable Management of Basalt in Clay Brick Industry after Its Application in Heavy Metals Removal. *J. Mater. Res. Technol.* **2021**, *10*, 1493–1502. [CrossRef]
31. Ziolli, R.L.; Jardim, W.F. Mechanism reactions of photodegradation of organic compounds catalyzed by TiO_2. *Quim Nova* **1998**, *21*, 319–325. [CrossRef]
32. Almeida, L.N.B.; Lenzi, G.G.; Pietrobelli, J.M.T.A.; Santos, O.A.A. Caffeine Degradation Using ZnO and Ag/ZnO under UV and Solar Radiation. *Desalination Water Treat* **2019**, *153*, 85–94. [CrossRef]
33. Mohammad-Rezaei, R.; Jaymand, M. Graphene Quantum Dots Coated on Quartz Sand as Efficient and Low-Cost Adsorbent for Removal of Hg^{2+} and Pb^{2+} from Aqueous Solutions. *Environ. Prog. Sustain. Energy* **2019**, *38*, S24–S31. [CrossRef]
34. Aguilera, J.G.; Zuffo, A.M.; Ratke, R.F.; Alves, C.Z.; Lima, R.E.; Nogueira, G.A.; de Aguiar, V.C.; de Oliveira, I.C.; dos Santos, M.D.; da Silva Cândido, A.C. Physiological Quality of Soybean Seeds in Response to Doses of Basalt Powder. *Res. Soc. Dev.* **2020**, *9*, e840986314. [CrossRef]
35. Almeida, L.N.; Josué, T.G.; Nogueira, O.H.; Dias, D.T.; Tusset, A.M.; Santos, O.A.; Lenzi, G.G. Quarry Residue: Treatment of Industrial Effluent Containing Dye. *Catalysts* **2021**, *11*, 852. [CrossRef]